BIOLOGY OF REPRODUCTION **84,** 966–975 (2011)
Published online before print 12 January 2011.
DOI 10.1095/biolreprod.110.090688

Analysis of *Nitroso*-Proteomes in Normotensive and Severe Preeclamptic Human Placentas[1]

Hong-hai Zhang,[3] Yu-ping Wang,[5] and Dong-bao Chen[2,3,4]

Departments of Obstetrics and Gynecology[3] and Experimental Pathology,[4] University of California Irvine, Irvine, California
Department of Obstetrics and Gynecology,[5] Louisiana State University Health Sciences Center, Shreveport, Louisiana

ABSTRACT

Nitric oxide (NO) plays a key role in placental biology, and placental dysfunction is the main pathogenesis pathway for preeclampsia, yet the direct placental targets of NO actions have not been determined. Covalent adduction of an NO moiety to cysteines, termed *S*-nitrosylation (SNO), is emerging as a key route by which NO can directly modulate protein functions. This study was conducted to analyze global *S-nitroso* (SNO)-proteins in human placentas and to determine if their levels differ in normotensive versus severe preeclamptic placentas. Although total nitrite/nitrate increased, total levels of SNO-proteins and nitrosylated forms of endothelial NO synthase and heat shock protein 90 were decreased by preeclampsia. We further compared normotensive and preeclamptic placental *nitroso*-proteomes (total SNO-protein profiles) by using a biotin and CyDye switch test combined with two-dimensional fluorescence difference gel electrophoresis (2D-DIGE) and identified SNO-proteins by matrix-assisted laser desorption/ionization time-of-flight mass spectrometry. Numerous SNO-proteins were displayed as spots on 2D-DIGE gels. One hundred spots of interest were excised; 46 spots were identified, of which 8 spots were novel SNO-proteins; levels of 15 spots were increased, and 6 spots were decreased, and the rest were unchanged by preeclampsia. Pathway analysis suggested that placental SNO-proteins are involved in regulating various cellular functions including protein synthesis, cell movement and metabolism, cell signaling, and other functions. These data therefore show for the first time that SNO is a crucial mechanism by which NO directly regulates placental proteins linked to various biological pathways. The significantly altered placental *nitroso*-proteome in preeclampsia suggests that SNO plays a role in the placental pathophysiology in preeclampsia.

nitric oxide, placenta, preeclampsia, proteomics, S-nitrosylation

INTRODUCTION

Preeclampsia complicates 5%–7% of all pregnancies worldwide and currently remains a major cause of maternal, fetal, and neonatal morbidity and mortality. It is diagnosed primarily by the onset of hypertension and proteinuria after 20 weeks of gestation. Severe preeclampsia is often complicated with the hemolysis, elevated liver enzymes, and low platelet count (HELLP) syndrome and/or fetal growth restriction [1]. The placenta has a central role in preeclampsia as evidenced by rapid disappearance of the disease symptoms after delivery or elective removal of the placenta but not the fetus [1]. Although the pathogenesis of preeclampsia is complex and still under intense investigation, endothelial dysfunction has been identified as a hallmark of preeclampsia [2, 3]. Most if not all of the theories proposed for the pathogenesis of preeclampsia are somewhat pointed to impaired spiral artery remodeling and insufficient trophoblast invasion [2]. Due to its potent vasodilator effects, nitric oxide (NO) plays a crucial role in lowering vascular resistance of the uterus and placenta unit throughout pregnancy. The decreased vascular resistance further enables local blood flow to rise to meet the growing needs of the fetus [4]. NO also regulates trophoblast function [5]. It is empirically accepted that pregnancy upregulates the NO system. This is important for pregnancy because inhibition of NO production generates preeclampsia-like symptoms in pregnant rats [6], and dysregulation of NO production is implicated in preeclampsia and intrauterine growth restriction [4]. Moreover, litter size is reduced in mice lacking the endothelial NO synthase (*Nos3*) gene [7]. However, it is noteworthy that the current understanding of NO biology in pregnancy remains principally at the stage of deciphering how NO is synthesized via the NOS family of isozymes including neuronal NOS (NOS1), inducible NOS (NOS2), and NOS3 by stimulation or pregnancy itself; how NO regulates placental protein functions and how this relates to placental biology and pregnancy are unknown.

Formation of cyclic guanylate monophosphate (cGMP) is the classical route by which NO elicits its biological functions [8]; however, many bioactivities of NO are now recognized as cGMP-independent [9]. NO is a gaseous molecule; its short half-life (~1 sec) makes its working distance relative short (~30 μm) [10]. Logically, endogenously synthesized NO can be trapped to act only within a few layers of cells; this favors endothelial cells for the action of NOS3-derived NO in an autocrine/paracrine fashion. However, once formed, NO can be quickly converted to reactive nitrogen species (RNS) such as N_2O_3, $ONOO^-$, NO_2^-, NO_3^-, and others [11]. These RNS can add a nitro (NO_2) group to the *ortho*-carbons of the aromatic ring of tyrosine; this is termed protein nitration [9], which has been linked to nitrosative stress in preeclamptic placentas [12, 13]. These RNS also can donate an NO moiety (NO•) to cysteines in a protein or peptide to produce *S*-nitrosothiols, which is termed *S*-nitrosylation (SNO) [14–16]. *S*-nitrosothiol possesses many NO-like biological functions but with a much longer biological half-life than NO [17, 18], serving as a reservoir for bioavailable NO [19]. This theory is of major importance in NO biology and medicine because this mechanism extends the biological functions of NO to an endocrine fashion so that NO can act on cells and/or organs far

[1]Supported in part by National Institutes of Health grants R21 HL98746, RO1 HL70562, and RO1 HL74947 (to D.-b.C.) and RO1 HD36822 (to Y.-p.W.).
[2]Correspondence: FAX: 949 824 2403; e-mail: dongbaoc@uci.edu

Received: 23 August 2010.
First decision: 6 October 2010.
Accepted: 4 January 2011.

eISSN: 1529-7268 http://www.biolreprod.org
ISSN: 0006-3363

from where it is produced [17]. SNO has a critical role in the cardiovascular system, as is clearly implicated in the phenotypes of mice lacking the major *S*-nitrosoglutathione (GSNO)-metabolizing enzyme GSNO reductase, ADH5. In *Adh5*$^{-/-}$ mice, GSNO turnover is required not only for preventing the accumulation of *S*-nitroso (SNO)-proteins that predisposes *Adh5*$^{-/-}$ mice to dysregulation of blood pressure, but also for regulating SNO turnover in the context of physiological signaling, which is especially important for regulation of blood pressure and vascular homeostasis [20, 21], as well as angiogenesis [22].

Although NO is important for the maintenance of normal pregnancy and *S*-nitrosylation represents a major route for NO to directly regulate protein functions, information on protein nitrosylation and its roles in placental biology is very limited. Dash et al. [24] reported that decreased caspase 3 activity via nitrosylation [23] is not linked to the protective effects of NO in human extravillous trophoblasts. However, they also showed that nitrosylation of proteins at the leading edge of migrating trophoblasts via NOS2 promotes trophoblast invasion [25]. In order to fully explore protein nitrosylation in human placenta and its implications in the pathogenesis of preeclampsia, our current study was designed to develop a comprehensive approach for analyzing human placental *nitroso*-proteomes (total SNO-protein profiles) and to test a hypothesis that SNO-protein targets and their levels were differentially altered in the placentas from normotensive and preeclamptic pregnancies.

MATERIALS AND METHODS

Chemicals

All chemicals were purchased from Sigma (St. Louis, MO) unless otherwise specified.

Placental Tissue Collection

Placentas were collected immediately after delivery from normal term (40 weeks) and severely preeclamptic pregnancies (n = 6/group) at Louisiana State University Health Sciences Center, Shreveport, LA (LSUHSC-S). Tissue collection was approved by the Institutional Review Board, with a waiver of consent from the LSUHSC-S. Villous tissue was isolated by sterile dissection. The tissue segments were washed thoroughly with cold phosphate-buffered saline (PBS) to remove blood from the intervillous spaces and then snap frozen in liquid nitrogen for storage at −80°C until assayed. The demographic data of the study subjects are summarized in Table 1. Severe preeclampsia was defined as maternal blood pressures of ≥160/110 mm Hg in two separate readings at least 6 h apart and significant quantitative proteinuria (≥3+ on urine dipstick or more than 2 g of total protein accumulated in a 24-h urine sample), as well as oliguria, cerebral or visual disturbances, pulmonary edema or cyanosis, epigastric or right upper-quarter pain, impaired liver function, thrombocytopenia, or fetal growth restriction. Smokers were excluded. None of the study subjects had prolonged rupture of membranes or signs of infection.

Total Nitrite/Nitrate (NO_2^-/NO_3^-) Assay

Levels of total NO_2^-/NO_3^- in placental homogenates were measured by using a nitrate/nitrite colorimetric assay kit (Cayman Inc., Ann Arbor, MI). Placental tissue samples (~20 mg each) were homogenized in PBS (pH 7.4) and centrifuged at 10 000 × *g* for 20 min. The supernatant was collected, and protein content was determined by using a bicinchoninic acid protein assay kit (Thermo Scientific, Rockford, IL). The homogenates were further filtered by using a 10-kDa molecular mass cutoff filter (Millipore, Billerica, MA) to remove large molecules before NO_2^-/NO_3^- measurement. The levels of total NO_2^-/NO_3^- were calculated according to a standard curve generated with sodium nitrate. The results were normalized with total protein levels.

Biotin Switch Technique and Avidin Capture of SNO Proteins

SNO-proteins were determined by using a SNO protein detection assay kit (Cayman Inc.) following the manufacturer's instructions. Placental tissue samples (~50 mg each) were homogenized in buffer A containing blocking reagent. Protein content was measured with a Bio-Rad procedure using bovine serum albumin as the standard. All samples were normalized to 0.3 mg/0.8 ml and then placed in 1.5-ml amber Eppendorf tubes. After incubation in buffer A containing blocking reagent at 4°C in the dark for 30 min, the samples were clarified by centrifugation (10 min, 4°C). The supernatants were transferred into 2-ml tubes and mixed with precooled acetone (1:4, vol/vol), and total proteins were precipitated at −20°C for 2 h. After centrifugation, the pellet was resuspended in 0.8 ml of buffer B containing the reducing agent sodium ascorbate and *N*-[6-(biotinamido)hexyl]-3′-(2′-pyridyldithio)propionamide (biotin-HPDP) and further incubated at room temperature in the dark for 2 h on a rocker with gentle agitation. The proteins were acetone precipitated again as described above. The pellet was thoroughly dissolved in 200 µl of HENS buffer [250 mM 4-(2-hydroxyethyl)-1-piperazineethanesulfonic acid (HEPES), pH 7.7, 1 mM ethylenediaminetetraacetic acid (EDTA), 0.1 mM neocuproine, 1% sodium dodecyl sulfate (SDS)], and then neutralized by adding 400 µl of neutralization buffer (20 mM HEPES, pH 7.7, 100 mM NaCl, 1 mM EDTA, 0.5% Triton X-100). A portion of the samples was saved for immunoblotting of total SNO-proteins with anti-biotin antibody. The rest (~0.25 mg/sample) was mixed with 50 µl of NeutrAvidin protein-coated beads (Thermo Scientific) and incubated at room temperature for 6 h. The beads were thoroughly washed with buffer C (20 mM HEPES, pH 7.7, 600 mM NaCl, 1 mM EDTA, 0.5% Triton X-100). The avidin-captured biotinylated SNO-proteins were eluted from the beads with 100 µl of 1× SDS sample buffer containing 1 mM dithiothreitol (DTT) at 37°C for 20 min and then analyzed for specific proteins of interest by immunoblotting, as described below.

TABLE 1. Demographic data of the pregnant study subjects used in the study.

Variables	Normotensive (n = 6)[a]	Preeclampsia (n = 6) [a]	*P* value
Maternal age (yr)	23 ± 6	24 ± 6	>0.50
Racial status			
White	0	2	–
Black	5	4	–
Other	1		
Gestational age (wk)	40 ± 1	34 ± 6	<0.05
Blood pressure (mm Hg)			
Systolic	119 ± 7	171 ± 23	<0.01
Diastolic	68 ± 8	109 ± 11	<0.01
Mode of delivery			
Vaginal	2	3	–
Caesarean section	4	3	–

[a] Values are mean ± SD; n = number of placentas per group.

SDS-PAGE and Immunoblotting for SNO Proteins

Protein samples were dissolved in 1× SDS sample buffer without DTT or β-mercaptoethanol and boiled for 5 min. Proteins were separated using 8% SDS-PAGE and transferred onto polyvinylidene fluoride (PVDF) membranes and immunoblotted with anti-biotin antibody (Cell Signaling, Beverly, MA). All SNO-proteins in each lane were summed for the level of SNO-proteins of the sample. Individual SNO-proteins were measured by immunoblotting of the avidin-captured biotinylated SNO-proteins by specific antibody, including anti-NOS3 (Santa Cruz Biotechnology, Santa Cruz, CA), anti-HSP90 (Invitrogen BD, Carlsbad, CA), and anti-β-actin (Ambion, Austin, TX).

CyDye Switch and Two-Dimensional Difference in Gel Electrophoresis

After blocking free thiols in the total protein extracts of the placental samples by using the biotin switch technique (BST) described above, 100 µg of total proteins sample was resuspended in 30 µl of reducing buffer (30 mM Tris-HCl, pH 8.0, 7 M urea, 2 M thiourea, 4% 3-[(3-cholamidopropyl)dimethylammonio]-1-propane-sulfonate, 1 mM sodium ascorbate). Following incubation at 37°C in the dark for 1 h, 4 µl of 2 mM CyDye two-dimensional difference in gel electrophoresis (2D-DIGE) saturation dyes (GE Healthcare, Buckinghamshire, U.K.) were added to the reaction mixtures (Cy3-normal and Cy5-preeclampsia, separately) and mixed well. The samples were further incubated at 37°C for 30 min in the dark, and 35 µl of 2 × 2D sample buffer was added and mixed. The samples were immediately stored at −70°C until 2D-DIGE was performed. The CyDye (Cy3 and Cy5) switched samples were mixed just before 2D-DIGE sample loading. For analytical 2D-DIGE, 50 µg of

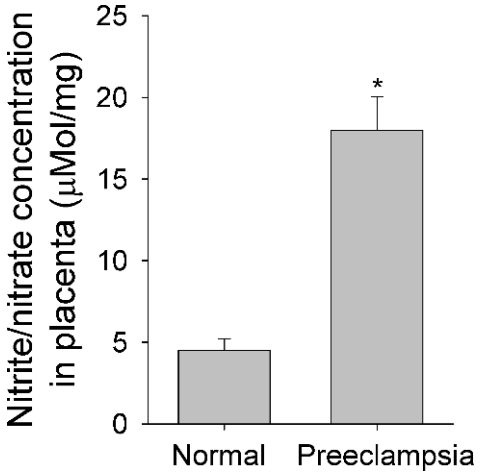

FIG. 1. Nitrite/nitrate concentrations are compared in normotensive and preeclamptic placentas. Placental nitrite (NO_2^-) and nitrate (NO_3^-) were measured with nitrate reductase, using a nitrate/nitrite colorimetric assay kit following the manufacturer's instructions (Cayman Inc.). Graphs summarize data (means ± SEM, n = 6) and compare by *t*-test. * $P <$ 0.05 vs. normal control.

proteins was loaded; for mass spectrometric analysis, 200 μg of proteins was loaded. The 2D-DIGE was performed by the commercial services of Applied Biomics, Inc. (http://www.Appliedbiomics.com/). After electrophoresis, the gel was scanned with both Cy3 and Cy5 channels, using a Typhoon image scanner (GE Healthcare). ImageQuant software (GE Healthcare) was used to generate the image presentation data including the single and overlay images, which were subjected to DeCyder software analysis (GE Healthcare). A ratio of the relative Cy5:Cy3 fluorescence intensities of the same spot was calculated based on an algorithm to adjust the difference of the loaded SNO-proteins in the paired samples.

Protein Identification by Matrix-Assisted Laser Desorption/Ionization-Time of Flight Mass Spectrometry

After 2D-DIGE and spot analysis using DeCyder software, spots of interest were chosen according to intensity and visibility and were excised from 2D gel with an Ettan Spot Picker (GE Healthcare). Each spot was trypsin digested and then analyzed using matrix-assisted laser desorption/ionization-time of flight mass spectrometry (MALDI-TOF-MS). The spectra (peptides) of each digested protein spot were subjected to a database search using GPS Explorer software with the MASCOT search engine (http://www.matrixscience.com) to identify proteins from the National Center for Biotechnology Information nonredundant *Homo sapiens* amino acid sequence database [26], with oxidation and carbamidomethyl and phosphorylation as variable modifications. The highest protein scoring hit with a protein score confidence interval (CI) of more than 95% from the database search for each 2D gel spot was accepted as positive identification.

Pathway Analysis and Statistics

An Ingenuity pathway analysis (www.ingenuity.com) tool was used to perform pathway analysis of the identified SNO-proteins. A positive result was defined as log (*P* value) > 1.30 ($P < 0.05$). Statistics were performed using SigmaStat version 3.5 software (Systat Software Inc., San Jose, CA). A Student *t*-test was used to compare data between normotensive and preeclamptic placentas. Significance was defined as a *P* value of <0.05.

RESULTS

NO_2^-/NO_3^- Concentrations in Normotensive and Preeclamptic Placentas

Total NO_2^-/NO_3^- has been widely used as an index of NO production in vivo [27]. Levels of NO_2^-/NO_3^- in the placental samples were measured to determine if placental NO production in preeclampsia differs from that in normotensive

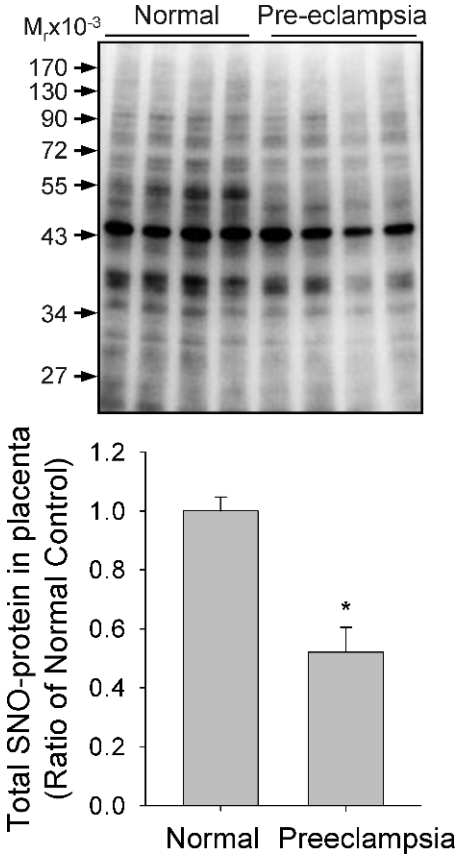

FIG. 2. Detection of SNO-proteins in normotensive and preeclamptic placentas using SDS-PAGE is shown. Placental homogenates were prepared and subjected to the biotin switch reaction. The biotin-labeled SNO-proteins were detected by using 8% SDS-PAGE and immunoblotted with an anti-biotin antibody. The same amounts of total protein were loaded in each lane. Four samples of each group were analyzed. Graphs summarize data (means ± SEM) and compare by *t*-test. * $P < 0.05$ vs. normal control.

controls. The levels of NO_2^-/NO_3^- in preeclamptic placentas were more than 4-fold greater ($P <0.05$) than in normotensive controls (Fig. 1).

Protein S-Nitrosylation in the Placenta

In addition to NO_2^-/NO_3^-, *S*-nitrosothiols have also been identified as major NO-related products in biological systems [17]. More recently, formation of *S*-nitrosothiols, defined as S-nitrosylation, has been rapidly moving to the center stage of cell signaling [28]. We used the BST to determine the total levels of placental SNO-proteins in both normotensive and preeclamptic pregnancies. The same amounts of placental homogenates were subjected to the BST, and the biotinylated proteins (hence SNO-proteins) were detected via immunoblotting with anti-biotin antibody. As shown in Figure 2, the levels of total SNO-proteins decreased significantly in preeclamptic placentas compared to those in normotensive placentas. Also of note, the intensities of several bands (SNO-proteins) were altered by preeclampsia. Because nitrosylation of NOS3 and its regulatory protein, heat shock protein 90 (HSP90), decrease NOS3 enzymatic activity [29], we further measured the levels of SNO-NOS3 and SNO-HSP90 that are important for NO biosynthesis. After BST was carried out, total SNO-proteins

were captured by avidin resins and then subjected to immunoblotting with antibodies against NOS3 or HSP90 to specifically determine the levels of nitrosylated forms of NOS3 and HSP90. Levels of nitrosylated forms of both NOS3 and HSP90 were significantly lower in placentas from preeclamptic pregnancies than in those from normotensive controls. In these samples, total NOS3 and HSP90 levels did not differ between the two groups. Levels of β-actin, measured as sample loading control, did not differ between the two groups; however, nitrosylated β-actin was lower in preeclamptic placentas (Fig. 3).

CyDye Switch/2D-DIGE Analysis of Placental Nitroso-*Proteome*

Based on results from the original BST [30], we have recently developed a powerful proteomic approach using CyDye Switch combined with 2D-DIGE (CyDye Switch/2D-DIGE) for analyzing *nitroso*-proteomes [31]. Cy3 (green) and Cy5 (red) DIGE fluorophores were used to replace the NO group in the SNO-proteins in normotensive and preeclamptic placentas, respectively. Following 2D electrophoresis, the resulting gel was scanned in both the Cy3 and the Cy5 channels. The relative fluorescence intensities of the spots of interest were calculated as ratios of the Cy3-labeled normotensive and Cy5-labeled preeclamptic placentas and are summarized in Table 2. Representative 2D-DIGE images of paired normotensive and preeclamptic placentas are shown in Figure 4, which were also reproduced with two additional pairs of samples (see Supplemental Fig. S1, available online at www.biolreprod.org). Many fluorescent spots (SNO-proteins) were visualized on the 2D-DIGE gel. As expected, many proteins were readily nitrosylated in placentas from both groups, and the levels of some were significantly altered by preeclampsia. The green spots on the 2D gel represent placental SNO-proteins whose levels of SNO were decreased by preeclampsia, whereas the red spots are placental SNO-proteins that were increased, and the yellow spots were unchanged by preeclampsia.

Because ascorbate at higher concentrations (>10 mM) has been shown to reduce disulfide bridges in low-molecular-weight thiols [32], we determined the effects of removing ascorbate from the labeling reaction mixture on total SNO-protein profiles labeled by biotin-HPDP under the buffer conditions of the original BST containing 0.4% 3-(3-cholamidopropyl) dimethylammonio-1-propanesulfonate [30] and 2.5% SDS or CyDye switch containing 7 M urea and 2 M thiourea [31, 33, and current study]. As shown in Figure 5, the total SNO-protein profiles were quite similar under these conditions, although the intensities of some SNO-proteins differed among different labeling conditions. Moreover, addition of 1 mM DDT to reduce disulfide bridges resulted in markedly increased nonspecific labeling. These data imply that 1 mM ascorbate specifically reduces the S-NO bond under the CyDye switch conditions used in the current study, as it does in the original BST, without reducing disulfide bonds.

Identification of Placental SNO-Proteins by MALDI-TOF Tandem MS

According to the intensity and visibility of the spots on the 2D-DIGE image, as well as their changes associated with preeclampsia, we focused on 100 spots of interest. Levels of relative fluorescence of these SNO-proteins between normotensive and preeclamptic placentas were determined offline, using ImageQuant and DeCyder software, and then calculated.

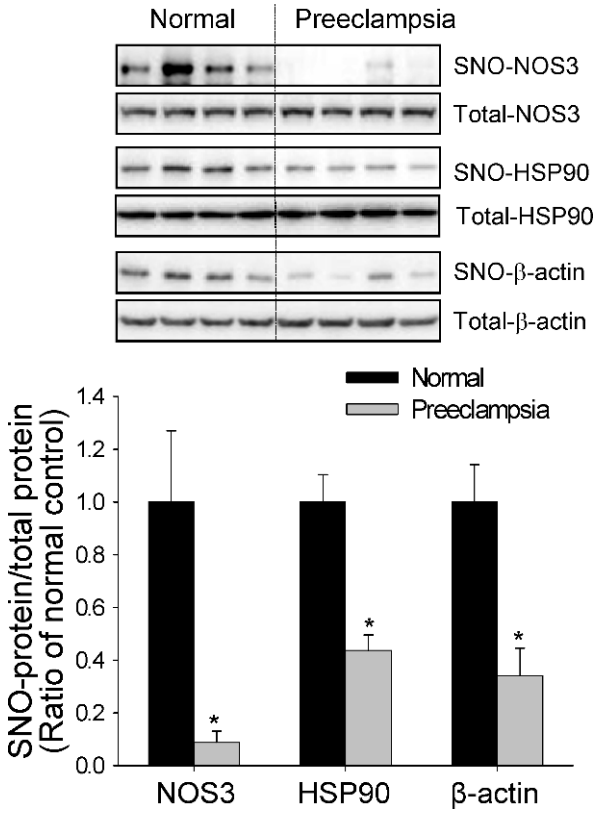

FIG. 3. *S*-nitrosylation of NOS3, HSP90, and β-actin in normotensive and preeclamptic placentas. The biotin-labeled SNO-proteins were further subjected to avidin capture. SNO-proteins, as well as total protein, were then separated by using 8% SDS-PAGE and immunoblotted with specific antibody. Four samples of each group were analyzed. Graph summarizes data (means ± SEM) and compares by *t*-test. * $P < 0.05$ vs. normal control.

Ratios whose levels of SNO were greater than 1 and with a P value of <0.05 represented spots upregulated by preeclampsia; whereas ratios ranging from 0 to 1 and with P of <0.05 represented spots decreased by preeclampsia. Based on these data, 200 μg of total proteins of both normotensive and preeclamptic placental samples were prepared by CyDye switch and run on newly prepared 2D-DIGE. After image acquisition, spots were matched with the analytic gel. The same 100 spots of interest on the new preparative gel were picked up. Each of the 100 spots picked up was in-gel digested with trypsin and then subjected to MALDI-TOF tandem MS (MS/MS). Spot identification was performed based on peptide fingerprinting MS/MS spectra with the Mascot algorithm searching in the National Center for Biotechnology Information nonredundant *Homo sapiens* amino acid sequence database. Using a CI greater than 95%, we identified 46 of the 100 spots subjected to MS/MS analysis. All peptides that matched each of these spots are listed in Supplemental Table S1 (available online at www.biolreprod.org). The identification of these SNO-proteins is summarized in Table 2, in which ratios between the relative levels of all 46 identified SNO-proteins are listed. Among the 46 SNO-proteins identified, expression levels of 15 SNO-proteins were significantly decreased, those of 6 SNO-proteins were decreased, and expression levels of the rest were unchanged by preeclampsia. Of note, we also identified eight novel SNO-proteins that have never been reported to date.

TABLE 2. Human placental SNO-proteins identified by two-dimensional fluorescence difference gel electrophoresis (2D-DIGE) and matrix assisted laser desorption/ionization-time of flight (MALDI-TOF)/tandem mass spectrometry.[a]

Spot no.	Protein name (symbol)	NCBI GENE-ID	MW (Da)/PI	No. peptides matched	Protein score	Ratio (PE/NC)[b]	*P* value[c]
1	Annexin A2 (ANXA2)	302	38,552/7.57	15	248	0.60 ± 0.15	**0.009**
2	Keratin 19 (KRT19)	3880	45,587/5.11	26	356	0.63 ± 0.11	**0.005**
3	Heat shock 70kDa protein 5 (glucose-regulated protein, 78kDa) (HSPA5)	3309	72,288/5.07	25	375	0.64 ± 0.11	**0.005**
4	Tyrosine 3-monooxygenase/tryptophan 5-monooxygenase activation protein, zeta polypeptide (YWHAZ)	7534	29,929/4.72	14	263	0.66 ± 0.12	**0.007**
5	GDP dissociation inhibitor 2 (GDI2)	2665	50,631/6.11	13	79	0.69 ± 0.11	**0.008**
6	Peroxiredoxin 1 (PRDX1)	5052	18,964/6.41	9	131	0.70 ± 0.11	**0.009**
7	Annexin A5 (ANXA5)	308	35,940/4.94	17	317	0.72 ± 0.13	**0.019**
8	Aconitase 2, mitochondrial (ACO2)	50	85,372/7.36	16	244	0.72 ± 0.15	**0.033**
9	Tropomyosin 2 (beta) (TPM2)	7169	32,970/4.63	16	148	0.73 ± 0.08	**0.005**
10	Voltage-dependent anion channel 2 (VDAC2)	7417	30,393/6.81	6	76	0.76 ± 0.05	**0.001**
11	Protein kinase C substrate 80K-H (PRKCSH)[d]	5589	59,141/4.34	16	172	0.77 ± 0.12	**0.029**
12	Actin, beta (ACTB)	60	40,194/5.55	10	98	0.78 ± 0.07	**0.006**
13	Tu translation elongation factor, mitochondrial (TUFM)	7284	49,843/7.26	10	80	0.79 ± 0.12	**0.041**
14	Heat shock protein 90kDa alpha (cytosolic), class A member 1 (HSP90AA1)	3320	84,607/4.94	24	382	0.82 ± 0.07	**0.013**
15	Enolase 1, (alpha) (ENO1)	2023	47,139/7.01	10	165	0.83 ± 0.05	**0.004**
16	Clathrin, light chain (CLTB)[d]	1212	25,175/4.57	9	185	0.73 ± 0.21	0.087
17	Heat shock protein 90kDa beta (Grp94), member 1(HSP90B1)	7184	92,411/4.76	17	156	0.80 ± 0.21	0.174
18	Chloride intracellular channel 1 (CLIC1)	1192	26,907/5.02	7	153	0.82 ± 0.19	0.167
19	Enoyl Coenzyme A hydratase 1, peroxisomal (ECH1)	1891	35,735/8.47	6	71	0.83 ± 0.19	0.195
20	Prolyl 4-hydroxylase, beta polypeptide (P4HB)	5034	57,069/4.82	19	474	0.83 ± 0.23	0.281
21	Isocitrate dehydrogenase 2 (NADP+), mitochondrial (IDH2)[d]	3418	50,877/8.88	13	86	0.84 ± 0.15	0.138
22	Protein disulfide isomerase family A, member 3 (PDIA3)	2923	56,761/5.98	17	181	0.86 ± 0.14	0.177
23	Transketolase (TKT)	7086	67,835/7.58	15	154	0.87 ± 0.16	0.221
24	Glutamate dehydrogenase 1(GLUD1)	2746	61,359/7.66	10	58	0.89 ± 0.33	0.579
25	Peroxiredoxin 1 (PRDX1)	5052	18,964/6.41	7	118	0.92 ± 0.26	0.603
26	Vimentin (VIM)	7431	53,681/5.03	25	404	0.92 ± 0.27	0.625
27	Hypoxia up-regulated 1 (HYOU1)[d]	10525	111,266/5.16	20	85	0.94 ± 0.45	0.837
28	Phosphoglycerate kinase 1 (PGK1)	5230	44,586/8.30	10	108	0.96 ± 0.08	0.476
29	Transferrin (TF)	7018	77,030/6.97	21	213	1.01 ± 0.37	0.976
30	Transgelin 2 (TAGLN2)	8407	21,073/7.63	8	81	1.02 ± 0.54	0.952
31	Albumin (ALB)	213	69,181/5.99	22	257	1.07 ± 0.07	0.158
32	Superoxide dismutase 1, soluble (SOD1)	6647	15,792/8.44	4	66	1.12 ± 0.37	0.604
33	Family with sequence similarity 82, member B (FAM82B)[d]	51115	35,785/8.64	6	41	1.18 ± 0.32	0.396
34	Peptidylprolyl isomerase A (cyclophilin A) (PPIA)	5478	18,000/7.68	9	358	1.19 ± 0.46	0.516
35	Peptidylprolyl isomerase A (cyclophilin A) (PPIA)	5478	18,000/7.68	8	86	1.21 ± 0.45	0.467
36	Chorionic somatomammotropin hormone 1 (placental lactogen) (CSH1)[d]	1442	22,294/5.33	10	165	1.25 ± 0.27	0.186
37	Peptidylprolyl isomerase A (cyclophilin A) (PPIA)	5478	18,000/7.68	8	136	1.31 ± 0.38	0.228
38	Calpain 6 (CAPN6)[d]	827	74,529/6.62	10	60	1.33 ± 0.38	0.209
39	Apolipoprotein A-1 (APOA1)[d]	335	30,759/5.56	17	310	1.35 ± 0.50	0.288
40	Pyruvate kinase, muscle (PKM2)	5315	57,942/7.96	15	162	1.38 ± 0.43	0.201
41	Heat shock 27kDa protein 1 (HSPB1)	3315	22,313/7.83	8	81	1.31 ± 0.09	**0.004**
42	Annexin A2 (ANXA2)	302	38,594/7.57	19	537	1.34 ± 0.10	**0.004**
43	Catalase (CAT)	847	59,719/6.90	13	111	1.60 ± 0.16	**0.003**
44	Annexin A2 (ANXA2)	302	40,386/8.53	13	124	1.80 ± 0.49	**0.047**
45	Carbonic anhydrase I (CA1)	759	28,852/6.59	10	103	2.03 ± 0.18	**<0.001**
46	Glyceraldehyde-3-phosphate dehydrogenase (GAPDH)	2597	36,031/8.26	7	65	2.28 ± 0.65	**0.027**

[a] NC, normotensive; PE, preeclampsia; MW, molecular weight; Da, Dalton; PI, isoelectric point.
[b] Values are mean ± SD.
[c] Statistics were performed using *t*-test, and significance was defined as $P < 0.05$ (values in bold indicate a significant change).
[d] Reported for the first time in this study as *S*-nitrosylated in vivo.

Pathway Analysis of Placental SNO-Proteins

Pathway analysis was performed using Ingenuity software to explore the potential biological functions of the identified SNO-proteins in the placenta. As listed in Table 3, pathway analysis suggested that the SNO-proteins identified are associated with various basic cellular physiologies, including viability, metabolism, cell cycle, signaling, and gene expression; DNA replication, recombination, and repair; and energy production, molecular transport, migration, and other functions. Many SNO-proteins are enzymes critical to protein synthesis, folding, posttranslational modification, and degradation.

DISCUSSION

Although the pathogenesis and etiology of preeclampsia remain largely undetermined, vascular and endothelial dysfunction in women with preeclampsia have been well documented [2, 3]. Because physiological levels of NO possess potent vasodilator, anticoagulation, and anti-inflammatory effects, the role that NO plays in pregnancy and how impaired NO biosynthesis and metabolism contribute to the pathogenesis of preeclampsia have been investigated intensively during the last 2 decades. It has been generally accepted that total NO synthesis capacity increases in normal pregnancy [4]; however, the literature describing NO production in preeclampsia is not

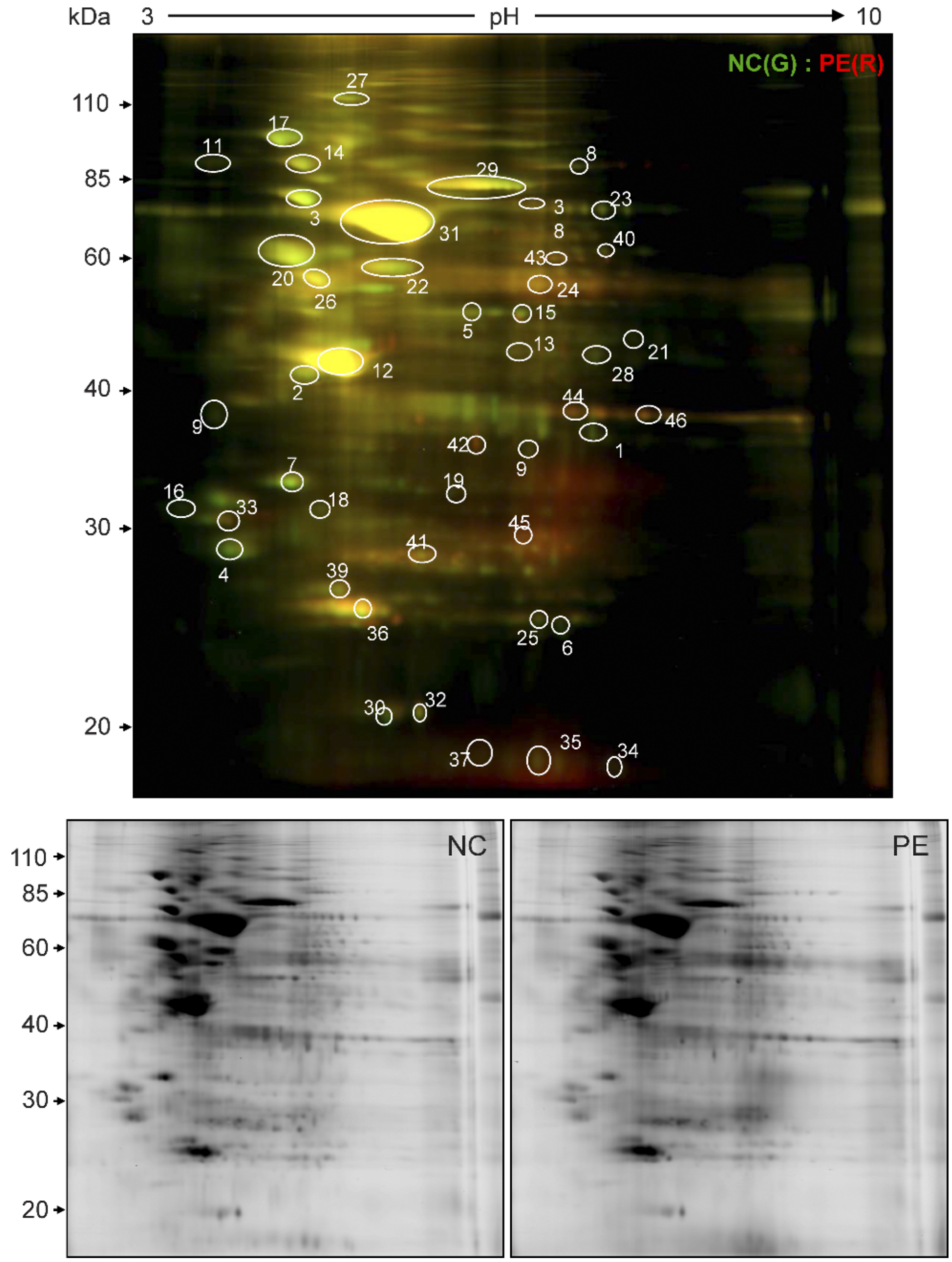

FIG. 4. Analysis of nitroso-proteomes in normotensive and preeclamptic placentas by CyDye switch/2D-DIGE. Total placental extracts (50 μg/sample) were assayed. Control samples were labeled with Cy3 (green), and preeclampsia samples were labeled with Cy5 (red). The samples were mixed (total, 100 μg) and then separated using analytical 2D-DIGE. The gel was scanned with a fluorescence scanner at different transmission and emission wavelengths for Cy3 (green, 548/560 nm) and Cy5 (red, 641/660 nm). The merged fluorescence image represents one of three separate experiments using samples from different placentas. Red, green, and yellow spots represent SNO-proteins that were increased, decreased, or unchanged by preeclampsia, respectively. The spots circled and numbered represent 46 SNO-proteins (Table 2), which were identified by MALDI-TOF-MS/MS. The black and white images represent fluorescent signals obtained from the red and green channels of one of the three experiments. NC, normotensive; PE, preeclampsia.

always consistent. Our data show that preeclampsia increases NO_2^-/NO_3^- concentration in placental tissues. This finding agrees with that of previous reports showing that circulating or placental levels of NO_2^-/NO_3^- increase in preeclampsia [34–39]; however, our finding contrasts to others showing decreased [40, 41] or unchanged [42, 43] placental NO production in preeclamptic compared to normal pregnancies.

Once formed, the short-lived NO can be quickly converted to other more stable metabolites such as NO_2^-/NO_3^- with very low bioactivity [27]. Thus, the total $NO_2^-:NO_3^-$ ratio has been widely used as an index of NO biosynthesis capacity in vivo. However, it is important to point out that NO also interacts with many other molecules to form relatively stable metabolites other than NO_2^-/NO_3^- such as proteins and metal ions [17]. For example, nitrosothiols represent an important class of stable NO derivatives that possess many NO-like biological activities. In biological systems, *S*-nitrosothiol formation and turnover may be of the greatest significance for the following reasons. First, interaction of NO with peptides or proteins may quench NO relative to its apoptotic effects when produced in excess [44]. Second, the relatively stable nitrosothiols can serve as a reservoir for NO, and when needed, NO can be released from this source to exert long-term biological activities [17]. Third, *S*-nitrosylation is a redox-sensitive and reversible posttranslational modification of proteins. Homologous to O-phosphorylation, *S*-nitrosylation regulates the activity of various proteins important for signal transduction [28]. Therefore, nitrosylation of proteins participates in the regulation of most if not all biological pathways [45]. Thus, in comparison to NO_2^-/NO_3^-, the level of *S*-nitrosothiols may be a more important indicator of NO bioavailability in vivo. We have found that the levels of total SNO-proteins are clearly decreased in preeclamptic compared to normotensive placentas. Meanwhile, significantly increased NO_2^-/NO_3^- in preeclamptic compared to normotensive placentas signifies that total NOS activity is increased in the preeclamptic placentas surveyed. However, decreased SNO-proteins in preeclamptic placentas suggest less bioavailable NO. Thus, it is possible that

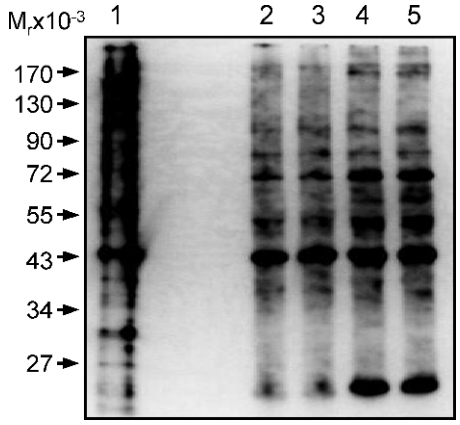

FIG. 5. Total SNO-protein profiles labeled with biotin-HPDP, using the labeling conditions of the original BST protocol and CyDye switch in the presence and absence of ascorbate. Equal amounts of total placental protein extracts were subjected to biotin switch for labeling total SNO-proteins under different conditions. Lane 1: samples were treated with 1 mM DDT and then subjected to biotin-HPDP labeling. Only 1 μg of total protein (1/20 of the other lanes) was loaded. Lane 2: original BST, without ascorbate removal before labeling; Lane 3: original BST, with ascorbate removal before labeling; Lane 4: BST using CyDye switch condition without ascorbate removal before labeling; Lane 5: BST using CyDye Switch condition with ascorbate removal before labeling. The proteins were resolved with 10% SDS-PAGE, transferred onto PVDF membranes, and then immunoblotted with an anti-biotin antibody.

even though NO biosynthesis may be increased in preeclampsia, most of the NO produced is metabolized as biologically inactive NO_2^-/NO_3^- [46, and current study]. Given the fact that oxidative stress is increased in preeclamptic placenta and that decreased NO bioavailability due to oxidative stress in endothelial cells leads to endothelial dysfunction [47], our data suggest that NO metabolism is impaired in the preeclamptic placenta, thereby contributing to the causes of endothelial and vascular dysfunction.

S-nitrosylation of proteins was first discovered by Stamler et al. [17], who found μM levels of SNO-albumin in circulating blood. However, research of protein nitrosylation has been hampered by difficulties in measuring the fragile *S*-NO bond until the BST was invented in 2001 [30]. In this method, the SNO group is first selectively reduced by ascorbate and then labeled with biotin, thus allowing SNO-proteins to be readily displayed, affinity purified, and identified. The specificity of this method has been recently confirmed [46]. Currently, this technique has been widely used for determining levels of nitrosothiols in various biological samples. Furthermore, several BST variants have been recently developed in which the biotin tag is replaced with fluorescent tags [33, 48, 49]. The fluorescently labeled SNO-proteins can either be visualized in situ by fluorescence microscopy [50] or they can be subjected to more powerful proteomic analysis such as 2D-DIGE [33]. The CyDye Switch/2D-DIGE method that we have developed offers a high-throughput proteomics approach to differentially display paired normotensive and preeclamptic placental *nitroso*-proteomes, as shown herein, and to identify the estrogen-responsive *nitroso* proteins in human umbilical vein endothelial cells [31]. Obviously, this method can be used for differential display of any paired *nitroso*-proteomes. However, our current method also has limitations because the same amounts of total proteins, but not SNO-proteins, from the paired samples were subjected to 2D-DIGE. The data obtained must be adjusted based on an algorithm to correct the difference of total SNO-proteins, and then a Cy5:Cy3 ratio of fluorescence intensities of the same spot is calculated to reflect the relative change in the protein between the samples. We are currently developing a method in which a fixed amount of a known protein nitrosylated in vitro is added at the labeling step as an internal control. This will assist data quantification and quality control of this system.

Although CyDye and Biotin-HPDP can be used for labeling SNO-proteins, these methods seem to have different affinities for each specific SNO-protein. For example, we have shown a major CyDye-labeled SNO-protein (Fig. 4, spot 31, albumin,

TABLE 3. Pathway analysis of the potential functionality of the human placental *S-nitroso*-proteins.

Biological functions	−Log (*P* value)[a]	*S-nitroso*-proteins identified
Protein degradation	5.74	CAT[b], HSP90B1, HSPA5[b]
Cell viability	1.44–4.94	ACTB[b], ALB, ANXA2[b], ANAXA5, APOA1, CAT[b], CSH1, ENO1[b], GAPDH[b], GLUD1, HSP90AA1[b], HSP90B1, HSPA5[b], HSPB1[b], HYOU1, KRT19[b], P4HB, PDIA3, PGK1, PKM2, PPIA, PRDX1[b], PRKCSH[b], SOD1, TF, TPM2[b], VDAC2[b], YWHAZ[b]
Small molecule biochemistry	1.35–5.26	ACO2[b], ALB, ANXA2[b], APOA1, CAT[b], CSH1, ECH1, GAPDH[b], GLUD1, HSP90B1, P4HB, PDIA3, PGK1, PPIA, PRDX1[b], PRKCSH[b], SOD1, TF, TKT, VIM, YWHAZ[b]
Free radical scavenging	1.64–5.23	ALB, CAT[b], HSPB1[b], PRDX1[b], PPIA, SOD1, TF
Cellular compromise and movement	1.41–3.84	ACTB[b], ALB, ANXA2[b], ANXA5[b], APOA1, CAT[b], CSH1, HSP90AA1[b], HSP90B1, HSPB1[b], PPIA, PRDX1[b], SOD1, VIM
Molecular transport and protein trafficking	1.36–3.75	ALB, APOA1, CAT[b], CLIC1, CSH1, GAPDH[b], HSP90AA1[b], HSPA5[b], HYOU1, PDIA3, PPIA, PRDX1[b], SOD1, TF, VDAC2[b], YWHAZ[b]
Metabolism	1.42–3.75	ALB, ANXA2[b], ANXA5[b], APOA1, CAT[b], CSH1, ECH1, ENO1[b], GAPDH[b], GLUD1, HSPA5[b], HYOU1, P4HB, PDIA3, PGK1, PKM2, PPIA, PRKCSH[b], SOD1, TKT, VIM
Protein synthesis	1.35–3.06	ANXA5[b], APOA1, CAT[b], HSPA5[b], HSPB1[b], PRKCSH[b], TUFM[b]
Post-translational modification		ALB, ANXA2[b], APOA1, CAT[b], GLUD1, HSP90AA1[b], HSPA5[b], P4HB, PDIA3, PPIA, PRDX1[b], SOD1,YWHAZ[b]
Protein folding	2.99	HSP90AA1[b], HSPA5[b], PPIA
DNA replication, recombination, and repair	1.42–2.70	CAT[b], HSPB1[b], PDIA3, PPIA, PRDX1[b], SOD1, VIM
Cell signaling	1.36–2.02	ALB, CAT[b], HSP90B1, HSPA5[b], HYOU1, PDIA3, PPIA, PRDX1[b], SOD1
Energy production	1.95	ACO2[b], ECH1
Gene expression	1.37–1.90	ALB, ENO1[b], PRDX1[b]

[a] The significance value associated with functional analysis for a dataset is a measure of the likelihood that the association between a set of functional analysis molecules in our experiment and a given process or pathway is due to random chance. The smaller the *P* value the less likely that the association is random and the more significant the association. In general, *P* values less than 0.05 indicate a statistically significant, non-random association. The *P* value is calculated using the right-tailed Fisher exact test.

[b] Protein with significantly altered *S*-nitrosylation level between normal and preeclampsia.

~69 kDa) using 2D-DIGE; SNO-albumin may come mainly from blood in the placental tissues. However, when labeled with biotin, this protein is not picked up by Western blotting with anti-biotin antibody (Fig. 2) as strongly as it is when labeled with CyDye. These results imply that CyDye and biotin have different affinities when labeling specific proteins. Also, it is possible that different proteins may have different affinities to the same labeling tag. This idea is supported by a report by Santhanam et al. [51], who used a mixture of known proteins including albumin to determine the efficiency of CyDye labeling. When a mixture composed of the same amounts of creatine kinase, bovine serum albumin, arginase I, and lysozyme was labeled with CyDye, the study found that albumin was labeled the strongest. Thus, both CyDye and Biotin-HPDP can be used to label SNO-proteins; however, the two methods seem to have different activities toward and affinities for each specific protein. Regardless, although each labeling method seems to have its own limitations, it is unlikely that the specific SNO-protein ratio between normotensive and preeclamptic placentas in our study is affected by using either the CyDye or the biotin labeling method.

S-nitrosylation alters enzyme activity by either modifying cysteines of the enzyme or changing protein conformation [28]. Of particular interest in the NOS3-NO system, we have determined the levels of SNO-NOS3 in placentas from both normotensive and preeclamptic pregnancies. We have found that both NOS3 and its stimulatory protein, HSP90 [52], were significantly less nitrosylated in preeclamptic placentas. Because nitrosylation inhibits the activity of NOS3 and HSP90 [29], these findings further support the notion that the NOS3-NO system may be more active in preeclampsia, in which decreased nitrosylation of NOS3 and HSP90 provides a compensatory mechanism against the overall decreased NO bioavailability.

In the partial placental *nitroso*-proteomes identified herein, we have found that the expression levels of 15 SNO-proteins are lowered and that of 6 other SNO-proteins are increased by preeclampsia. Among these proteins are the peroxiredoxins (PRDXs), a family of ubiquitously expressed antioxidant enzymes that control intracellular superoxide levels, thereby affecting the participating signal transduction [53]. It has been reported that nitrosylation decreases the activity of PRDX, thereby lowering its antioxidant activity [54]. Of note, we have found that preeclampsia was associated with increased levels of SNO-PRDXs. Thus, our findings suggest that increased SNO-PRDXs contribute to increased oxidative stress commonly seen in preeclampsia [47]. Glyceraldehyde 3-phosphate dehydrogenase (GAPDH) is a metabolic enzyme required for glycolysis, and nitrosylation of GAPDH has been linked to NO-induced apoptotic death [55]. Annexin, keratin, and β-actin are cytoskeleton proteins that are involved in cell migration; denitrosylation of these three proteins may be related to the inadequate trophoblast invasion in preeclampsia [56]. SNO-NOS3 is not identified in the partial *nitroso*-proteome, possibly due to its low abundance. However, SNO-HSP90 has been identified as a downregulated SNO-protein in the placental *nitroso*-proteome. This is consistent with the combined BST and avidin capture assay (Fig. 3).

We also have identified eight novel SNO-proteins that have never been reported to date (Table 2). Apolipoprotein A-1 is the major protein component of high-density lipoproteins present in the plasma; it has a specific role in lipid metabolism [57]. Calpains are calcium-dependent cysteine proteases that are involved in signal transduction in a variety of cellular processes; for example, Calpain 6 might play a role in sex determination [58]. Human chorionic somatomammotropin is a polypeptide placental hormone; it modifies the metabolic state of the mother during pregnancy to facilitate energy supply to the fetus and has anti-insulin activities [59]. Hypoxia-upregulated protein 1 (also known as ORP150) belongs to the heat shock protein 70 family; overexpression of ORP150 in cultured neurons prevents cell apoptosis from hypoxemic stress [60]. Isocitrate dehydrogenases are enzymes that catalyze the oxidative decarboxylation of isocitrate to 2-oxoglutarate and participate in the citric acid cycle [61]. Clathrin facilitates the formation of small vesicles in the cytoplasm; clathrin-coated vesicles selectively sort cargo at the cell membrane, trans-Golgi network, and endosomal compartments for multiple membrane traffic pathways [62]. Protein kinase C substrate 80K-H is an acidic phosphoprotein known to be a substrate for protein kinase C and is associated with autosomal dominant polycystic liver disease [63]. The specific function of family with sequence similarity 82 (FAM82B) protein has yet to be determined. However, the functional sequelae of nitrosylation of these proteins are unknown and waiting for further investigation.

We have identified spots 1, 42, and 44 on the 2D gel (Fig. 4) as belonging to the same protein, annexin A2. However, it is intriguing that they display different nitrosylation changes in the normotensive and preeclamptic placentas. Nitrosylation of spot 1 (Fig. 4) is significantly decreased (ratio = 0.75), whereas spots 42 and 44 (Fig. 4) are significantly increased (ratios are 1.34 and 1.80, respectively) by preeclampsia. Position shift of a protein on the 2D gel is usually a result of posttranslation modifications leading to a change in the isoelectric point of the protein [64]. Thus, these observations imply that preeclampsia can induce posttranslational modifications of proteins, such as changing the isoelectric point, which in turn leads to different outcomes in *S*-nitrosylation in placental proteins.

In summary, we have analyzed herein the *nitroso*-proteomes in normotensive and preeclamptic human placentas. Differential displays of the two *nitroso*-proteomes and pathway analysis of the potential function of the placental SNO-proteins identified imply that protein nitrosylation seems to play a critical role in regulating normal placental physiology and pathophysiology. This is because not only are numerous proteins nitrosylated in normotensive human placenta, but also the levels of a number of the placental SNO-proteins are altered by preeclampsia. To the best of our knowledge, our current study is the first to take a comprehensive proteomics approach for analyzing the global changes in protein nitrosylation in the placenta. Although the functional sequelae of the nitrosylated proteins identified in the current study and whether changes in SNO-proteins contribute to the pathogenesis of preeclampsia need to be determined, our current study signifies a critical next step in identifying the direct targets that are affected by NO in the placenta. We believe that further investigations of the functional sequelae of protein nitrosylation will be critical for advancing knowledge of NO biology in pregnancy.

REFERENCES

1. Roberts JM, Cooper DW. Pathogenesis and genetics of pre-eclampsia. Lancet 2001; 357:53–56.
2. Redman CW, Sargent IL. Latest advances in understanding preeclampsia. Science 2005; 308:1592–1594.
3. Roberts JM, Hubel CA, Taylor RN. Endothelial dysfunction yes, cytotoxicity no! Am J Obstet Gynecol 1995; 173:978–979.
4. Sladek SM, Magness RR, Conrad KP. Nitric oxide and pregnancy. Am J Physiol 1997; 272:R441–R463.
5. Sanyal M, Nag TC, Das C. Localization of nitric oxide synthase in human trophoblast cells: role of nitric oxide in trophoblast proliferation and differentiation. Am J Reprod Immunol 2000; 43:70–77.
6. Buhimschi I, Yallampalli C, Chwalisz K, Garfield RE. Pre-eclampsia-like

conditions produced by nitric oxide inhibition: effects of L-arginine, D-arginine and steroid hormones. Hum Reprod 1995; 10:2723–2730.
7. van der Heijden OW, Essers YP, Fazzi G, Peeters LL, De Mey JG, van Eys GJ. Uterine artery remodeling and reproductive performance are impaired in endothelial nitric oxide synthase-deficient mice. Biol Reprod 2005; 72:1161–1168.
8. Denninger JW, Marletta MA. Guanylate cyclase and the NO/cGMP signaling pathway. Biochim Biophys Acta 1999; 1411:334–350.
9. Wanstall JC, Homer KL, Doggrell SA. Evidence for, and importance of, cGMP-independent mechanisms with NO and NO donors on blood vessels and platelets. Curr Vasc Pharmacol 2005; 3:41–53.
10. Smith KM, Moore LC, Layton HE. Advective transport of nitric oxide in a mathematical model of the afferent arteriole. Am J Physiol Renal Physiol 2003; 284:F1080–F1096.
11. Radi R, Peluffo G, Alvarez MN, Naviliat M, Cayota A. Unraveling peroxynitrite formation in biological systems. Free Radic Biol Med 2001; 30:463–488.
12. Webster RP, Brockman D, Myatt L. Nitration of p38 MAPK in the placenta: association of nitration with reduced catalytic activity of p38 MAPK in pre-eclampsia. Mol Hum Reprod 2006; 12:677–685.
13. Webster RP, Roberts VH, Myatt L. Protein nitration in placenta—functional significance. Placenta 2008; 29:985–994.
14. Stamler JS, Lamas S, Fang FC. Nitrosylation. The prototypic redox-based signaling mechanism. Cell 2001; 106:675–683.
15. Boehning D, Snyder SH. Novel neural modulators. Annu Rev Neurosci 2003; 26:105–131.
16. Foster MW, McMahon TJ, Stamler JS. S-nitrosylation in health and disease. Trends Mol Med 2003; 9:160–168.
17. Stamler JS, Simon DI, Osborne JA, Mullins ME, Jaraki O, Michel T, Singel DJ, Loscalzo J. S-nitrosylation of proteins with nitric oxide: synthesis and characterization of biologically active compounds. Proc Natl Acad Sci U S A 1992; 89:444–448.
18. Keaney JF Jr, Simon DI, Stamler JS, Jaraki O, Scharfstein J, Vita JA, Loscalzo J. NO forms an adduct with serum albumin that has endothelium-derived relaxing factor-like properties. J Clin Invest 1993; 91:1582–1589.
19. Reynaert NL, Ckless K, Wouters EF, van der Vliet A, Janssen-Heininger YM. Nitric oxide and redox signaling in allergic airway inflammation. Antioxid Redox Signal 2005; 7:129–143.
20. Liu L, Yan Y, Zeng M, Zhang J, Hanes MA, Ahearn G, McMahon TJ, Dickfeld T, Marshall HE, Que LG, Stamler JS. Essential roles of *S*-nitrosothiols in vascular homeostasis and endotoxic shock. Cell 2004; 116: 617–628.
21. Lima B, Forrester MT, Hess DT, Stamler JS. S-nitrosylation in cardiovascular signaling. Circ Res 2010; 106:633–646.
22. Lima B, Lam GK, Xie L, Diesen DL, Villamizar N, Nienaber J, Messina E, Bowles D, Kontos CD, Hare JM, Stamler JS, Rockman HA. Endogenous *S*-nitrosothiols protect against myocardial injury. Proc Natl Acad Sci U S A 2009; 106:6297–6302.
23. Mannick JB, Hausladen A, Liu L, Hess DT, Zeng M, Miao QX, Kane LS, Gow AJ, Stamler JS. Fas-induced caspase denitrosylation. Science 1999; 284:651–654.
24. Dash PR, Cartwright JE, Baker PN, Johnstone AP, Whitley GS. Nitric oxide protects human extravillous trophoblast cells from apoptosis by a cyclic GMP-dependent mechanism and independently of caspase 3 nitrosylation. Exp Cell Res 2003; 287:314–324.
25. Harris LK, McCormick J, Cartwright JE, Whitley GS, Dash PR. S-nitrosylation of proteins at the leading edge of migrating trophoblasts by inducible nitric oxide synthase promotes trophoblast invasion. Exp Cell Res 2008; 314:1765–1776.
26. Pruitt KD, Tatusova T, Maglott DR. NCBI reference sequence (RefSeq): a curated non-redundant sequence database of genomes, transcripts and proteins. Nucleic Acids Res 2007; 35:D61–D65.
27. Lauer T, Preik M, Rassaf T, Strauer BE, Deussen A, Feelisch M, Kelm M. Plasma nitrite rather than nitrate reflects regional endothelial nitric oxide synthase activity but lacks intrinsic vasodilator action. Proc Natl Acad Sci U S A 2001; 98:12814–12819.
28. Lane P, Hao G, Gross SS. S-nitrosylation is emerging as a specific and fundamental posttranslational protein modification: head-to-head comparison with *O*-phosphorylation. Sci STKE 2001; (86):re1.
29. Ravi K, Brennan LA, Levic S, Ross PA, Black SM. S-nitrosylation of endothelial nitric oxide synthase is associated with monomerization and decreased enzyme activity. Proc Natl Acad Sci U S A 2004; 101:2619–2624.
30. Jaffrey SR, Snyder SH. The biotin switch method for the detection of S-nitrosylated proteins. Sci STKE 2001;(86):pl1.
31. Zhang HH, Feng L, Livnat I, Hoh JK, Shim JY, Liao WX, Chen DB. Estradiol-17(beta) stimulates specific receptor and endogenous nitric oxide-dependent dynamic endothelial protein S-nitrosylation: analysis of endothelial nitrosyl-proteome. Endocrinology 2010; 151:3874–3887.
32. Giustarini D, Dalle-Donne I, Colombo R, Milzani A, Rossi R. Is ascorbate able to reduce disulfide bridges? A cautionary note. Nitric Oxide 2008; 19: 252–258.
33. Huang B, Chen SC, Wang DL. Shear flow increases S-nitrosylation of proteins in endothelial cells. Cardiovasc Res 2009; 83:536–546.
34. Norris LA, Higgins JR, Darling MR, Walshe JJ, Bonnar J. Nitric oxide in the uteroplacental, fetoplacental, and peripheral circulations in preeclampsia. Obstet Gynecol 1999; 93:958–963.
35. Nobunaga T, Tokugawa Y, Hashimoto K, Kimura T, Matsuzaki N, Nitta Y, Fujita T, Kidoguchi KI, Azuma C, Saji F. Plasma nitric oxide levels in pregnant patients with preeclampsia and essential hypertension. Gynecol Obstet Invest 1996; 41:189–193.
36. Smarason AK, Allman KG, Young D, Redman CW. Elevated levels of serum nitrate, a stable end product of nitric oxide, in women with pre-eclampsia. Br J Obstet Gynaecol 1997; 104:538–543.
37. Bartha JL, Comino-Delgado R, Bedoya FJ, Barahona M, Lubian D, Garcia-Benasach F. Maternal serum nitric oxide levels associated with biochemical and clinical parameters in hypertension in pregnancy. Eur J Obstet Gynecol Reprod Biol 1999; 82:201–207.
38. Pathak N, Sawhney H, Vasishta K, Majumdar S. Estimation of oxidative products of nitric oxide (nitrates, nitrites) in preeclampsia. Aust N Z J Obstet Gynaecol 1999; 39:484–487.
39. Shaamash AH, Elsnosy ED, Makhlouf AM, Zakhari MM, Ibrahim OA, EL-dien HM. Maternal and fetal serum nitric oxide (NO) concentrations in normal pregnancy, pre-eclampsia and eclampsia. Int J Gynaecol Obstet 2000; 68:207–214.
40. Salas SP. Role of nitric oxide in maternal hemodynamics and hormonal changes in pregnant rats. Biol Res 1998; 31:243–250.
41. Mutlu-Turkoglu U, Aykac-Toker G, Ibrahimoglu L, Ademoglu E, Uysal M. Plasma nitric oxide metabolites and lipid peroxide levels in preeclamptic pregnant women before and after delivery. Gynecol Obstet Invest 1999; 48:247–250.
42. Silver RK, Kupferminc MJ, Russell TL, Adler L, Mullen TA, Caplan MS. Evaluation of nitric oxide as a mediator of severe preeclampsia. Am J Obstet Gynecol 1996; 175:1013–1017.
43. Egerman RS, Andersen RN, Manejwala FM, Sibai BM. Neuropeptide Y and nitrite levels in preeclamptic and normotensive gravid women. Am J Obstet Gynecol 1999; 181:921–923.
44. Messmer UK, Lapetina EG, Brune B. Nitric oxide-induced apoptosis in RAW 264.7 macrophages is antagonized by protein kinase C- and protein kinase A-activating compounds. Mol Pharmacol 1995; 47:757–765.
45. Hess DT, Matsumoto A, Kim SO, Marshall HE, Stamler JS. Protein S-nitrosylation: purview and parameters. Nat Rev Mol Cell Biol 2005; 6: 150–166.
46. Forrester MT, Foster MW, Stamler JS. Assessment and application of the biotin switch technique for examining protein S-nitrosylation under conditions of pharmacologically induced oxidative stress. J Biol Chem 2007; 282:13977–13983.
47. Myatt L, Cui X. Oxidative stress in the placenta. Histochem Cell Biol 2004; 122:369–382.
48. Sun J, Morgan M, Shen RF, Steenbergen C, Murphy E. Preconditioning results in S-nitrosylation of proteins involved in regulation of mitochondrial energetics and calcium transport. Circ Res 2007; 101:1155–1163.
49. Torta F, Usuelli V, Malgaroli A, Bachi A. Proteomic analysis of protein S-nitrosylation. Proteomics 2008; 8:4484–4494.
50. Yang Y, Loscalzo J. *S*-nitrosoprotein formation and localization in endothelial cells. Proc Natl Acad Sci U S A 2005; 102:117–122.
51. Santhanam L, Gucek M, Brown TR, Mansharamani M, Ryoo S, Lemmon CA, Romer L, Shoukas AA, Berkowitz DE, Cole RN. Selective fluorescent labeling of *S*-nitrosothiols (S-FLOS): a novel method for studying *S*-nitrosation. Nitric Oxide 2008; 19:295–302.
52. Martinez-Ruiz A, Villanueva L, Gonzalez de Orduna C, Lopez-Ferrer D, Higueras MA, Tarin C, Rodriguez-Crespo I, Vazquez J, Lamas S. S-nitrosylation of Hsp90 promotes the inhibition of its ATPase and endothelial nitric oxide synthase regulatory activities. Proc Natl Acad Sci U S A 2005; 102:8525–8530.
53. Rhee SG, Chae HZ, Kim K. Peroxiredoxins: a historical overview and speculative preview of novel mechanisms and emerging concepts in cell signaling. Free Radic Biol Med 2005; 38:1543–1552.
54. Fang J, Nakamura T, Cho DH, Gu Z, Lipton SA. S-nitrosylation of peroxiredoxin 2 promotes oxidative stress-induced neuronal cell death in Parkinson's disease. Proc Natl Acad Sci U S A 2007; 104:18742–18747.
55. Hara MR, Agrawal N, Kim SF, Cascio MB, Fujimuro M, Ozeki Y, Takahashi M, Cheah JH, Tankou SK, Hester LD, Ferris CD, Hayward SD,

et al. S-nitrosylated GAPDH initiates apoptotic cell death by nuclear translocation following Siah1 binding. Nat Cell Biol 2005; 7:665–674.
56. Goldman-Wohl D, Yagel S. Regulation of trophoblast invasion: from normal implantation to pre-eclampsia. Mol Cell Endocrinol 2002; 187: 233–238.
57. Brouillette CG, Anantharamaiah GM, Engler JA, Borhani DW. Structural models of human apolipoprotein A-I: a critical analysis and review. Biochim Biophys Acta 2001; 1531:4–46.
58. Huang Y, Wang KK. The calpain family and human disease. Trends Mol Med 2001; 7:355–362.
59. Strobl JS, Thomas MJ. Human growth hormone. Pharmacol Rev 1994; 46: 1–34.
60. Tamatani M, Matsuyama T, Yamaguchi A, Mitsuda N, Tsukamoto Y, Taniguchi M, Che YH, Ozawa K, Hori O, Nishimura H, Yamashita A, Okabe M, et al. ORP150 protects against hypoxia/ischemia-induced neuronal death. Nat Med 2001; 7:317–323.
61. Thauer RK. Citric-acid cycle, 50 years on. Modifications and an alternative pathway in anaerobic bacteria. Eur J Biochem 1988; 176:497–508.
62. Schmid SL. Clathrin-coated vesicle formation and protein sorting: an integrated process. Annu Rev Biochem 1997; 66:511–548.
63. Drenth JP, Tahvanainen E, te Morsche RH, Tahvanainen P, Kaariainen H, Hockerstedt K, van de Kamp JM, Breuning MH, Jansen JB. Abnormal hepatocystin caused by truncating PRKCSH mutations leads to autosomal dominant polycystic liver disease. Hepatology 2004; 39: 924–931.
64. Towbin H, Ozbey O, Zingel O. An immunoblotting method for high-resolution isoelectric focusing of protein isoforms on immobilized pH gradients. Electrophoresis 2001; 22:1887–1893.